PL ISSN 0209-0058 MATERIAŁY ELEKTRONICZNE T. 36 - 2008 NR 3

DIELECTRIC PROPERTIES OF PEROVSKITE MULTIFERROIC $Pb(Fe_{0.5}Nb_{0.5})O_3$-$Bi_{0.95}Dy_{0.05}FeO_3$ THICK FILMS*

Agata Stoch[1], Jan Kulawik[1], Dorota Szwagierczak[1], Barbara Gröger[1]

The paper reports the preparation and deposition of dielectric thick films exhibiting multiferroic properties. The developed layers are based on solid solutions of two multiferroic compounds with perovskite structure - relaxor $Pb(Fe_{0.5}Nb_{0.5})O_3$ and $Bi_{0.95}Dy_{0.05}FeO_3$. Complex impedance and dielectric permittivity of thick films were determined as a function of temperature (from –55 to 450°C) and frequency (10 Hz - 2 MHz). Dc resistivity was measured in the temperature range 20 – 400°C. Microstructure of the samples was studied using a scanning electron microscope. In complex plane impedance spectra there exists a single arc at a given temperature associated with grains which decreases and shifts to higher frequencies with increasing temperature. The maximum values of dielectric permittivity of the investigated layers were 2000 - 4000 in the temperature range from -55 to 150°C at 1 kHz. Two broad ε'maxima ascribed to relaxor ferroelectric transition and dielectric relaxation occur in the temperature range from -55 to 450°C. Low sintering temperature appropriate for the conventional thick film procedure, dense microstructure and high dielectric permittivity slightly changing over a wide frequency and temperature ranges are advantages of the developed compositions.

***Key words**:* perovskite multiferroics, thick films, dielectric properties
***Słowa kluczowe**:* perowskitowe multiferroiki, warstwa gruba, właściwości dielektryczne

[1] Instytut Technologii Elektronowej, Oddział w Krakowie, ul. Zabłocie 39, 30-701 Kraków; Corresponding autor email: jkulawik@ite.waw.pl

* Praca prezentowana na XXXII International Conference of IMAPS - CPMP IEEE Poland, Pułtusk, 21-24.09.2008

1. INTRODUCTION

Multiferroics exhibiting simultaneously ferroelectric and ferromagnetic properties have recently attracted great attention as promising intelligent multifunctional materials for various applications such as: memories, actuators, sensors, oscillators, etc. Two approaches are available - use of single-phase multiferroic compounds or application of composite materials composed e.g. of perovskite ferroelectric and spinel ferromagnetic ($BaTiO_3$–$CoFe_2O_4$, $PbTiO_3$–$NiFe_2O_4$, $BaTiO_3$-$Ni_{0.5}Zn_{0.5}Fe_2O_4$).

One of the most interesting group of single-phase multiferroic materials are those with perovskite structure, like $BiFeO_3$ and relaxors: $Pb(Fe_{1/2}Nb_{1/2})O_3$, $Pb(Fe_{1/2}Ta_{1/2})O_3$ and $Pb(Fe_{2/3}W_{1/3})O_3$ [1-11]. Among these compounds, $BiFeO_3$ is the most extensively studied [4-6] due to its multiferroic properties at room temperature (ferroelectric transition at 827°C and antiferromagnetic transition at 367°C). Low melting temperature (930°C), unstable structure and high leakage current are disadvantages of $BiFeO_3$. Overcoming of these problems may be attained in solid solutions of this compound with other perovskite materials with more stable structure, higher resistivity and higher sintering temperatures (e.g. $BaTiO_3$, $PbTiO_3$, relaxors). Partial substitution of Bi ions by isovalent ions, like La, Nd, Pr, Dy, and/or Fe ions by Sc can also improve the properties of $BiFeO_3$.

$Pb(Fe_{1/2}Nb_{1/2})O_3$ is a relaxor ferroelectric with diffuse ferroelectric transition at 112°C and antiferromagnetic transition at -130 to -103°C [7,8]. Sintering temperatures of ceramics based on this compound are about 1100°C.

The subject of this paper is fabrication and characterization of thick films based on solid solutions of two multiferroic compounds with perovskite structure - relaxor $Pb(Fe_{1/2}Nb_{1/2})O_3$ and $BiFeO_3$ doped with 5 mol % Dy_2O_3. The present work is focused on the investigation of dielectric response of the layers. The magnetic properties of the considered materials in the ceramic form have been presented elsewhere [11] and these studies are planned to be continued in future works.

2. EXPERIMENTAL

The two-step "wolframite" synthesis method was used to synthesize $Pb(Fe_{1/2}Nb_{1/2})O_3$ (PFN). During the first calcination step Fe_2O_3 reacted with Nb_2O_5 at 1000°C for 4 h, during the second step $FeNbO_4$ (with wolframite structure) reacted with PbO at 800°C for 4 h. Addition of 0.5 - 1 mol % of MnO_2 was applied in order to improve resistivity of this material. $Bi_{0.95}Dy_{0.05}FeO_3$ (BDF) was synthesized by calcination at 900°C for 5 h. Three compositions: 0.5PFN-0.5BDF, 0.7PFN-0.3BDF and 0.9PFN-0.1BDF were mixed in appropriate proportions, ball-milled, pressed into discs and calcined at 850°C to form solid solutions. The synthesis products were

ball-milled in isopropyl alcohol for 6 h. X-ray diffraction analysis confirmed single phase perovskite structure of 0.5PFN-0.5BDF ceramic samples [11].

The dielectric pastes were prepared by mixing the ceramic powders with 40 wt. % of the solution of ethyl cellulose in terpineol and subsequent grinding in an agate mortar. Thick film capacitors were screen printed on alumina substrates. Bottom and top electrodes were deposited using an Ag paste. The triple dielectric layers were screen printed, dried and fired in a VI-zone BTU belt furnace for 10 minutes at peak temperature of 830 - 850°C. The thickness of the dielectric layers examined by means of a profilograph was about 20 μm.

Complex impedance and dielectric permittivity of thick films were determined as a function of temperature (from –55 to 450°C) and frequency (from 10 Hz to 2 MHz) using a LCR QuadTech meter. Dc resistivity was measured in the temperature range 20 – 400°C by means of a Philips resistance meter. Microstructure of the samples and compatibility with silver electrodes was studied using a FEI scanning electron microscope.

3. RESULTS AND DISCUSSION

In Figs. 1-3 the real part of permittivity, temperature coefficient of capacitance (TCC) and dissipation factor are compared for 0.5PFN-0.5BDF, 0.7PFN-0.3BDF and 0.9PFN-0.1BDF thick films.

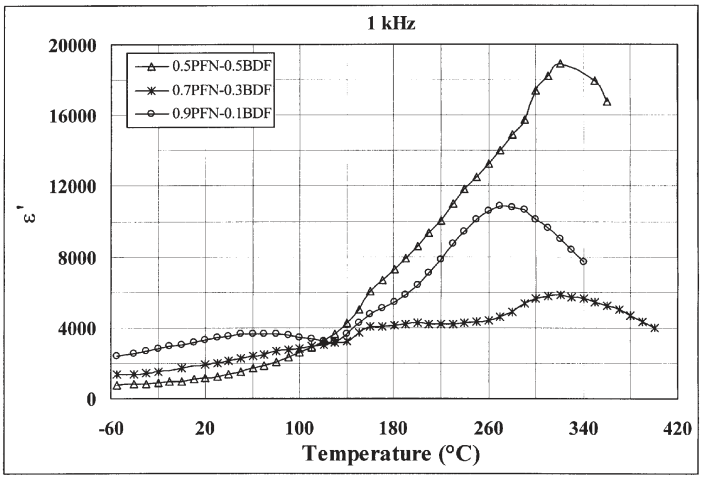

Fig. 1. Comparison of temperature dependences of the real part of permittivity at 1 kHz for 0.5PFN-0.5BDF, 0.7PFN-0.3BDF and 0.9PFN-0.1BDF thick films.
Rys. 1. Porównanie temperaturowych zależności części rzeczywistej przenikalności dla warstw warstw 0.5PFN-0.5BDF, 0.7PFN-0.3BDF i 0.9PFN-0.1BDF dla 1 kHz.

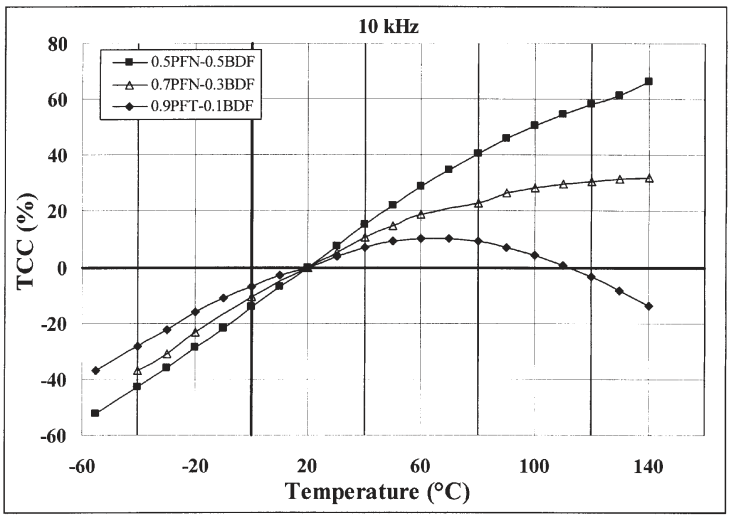

Fig. 2. Temperature coefficients of capacitance at 10 kHz for 0.5PFN-0.5BDF, 0.7PFN--0.3BDF and 0.9PFN-0.1BDF thick films.
Rys. 2. Temperaturowy współczynnik pojemności dla warstw grubych 0.5PFN-0.5BDF, 0.7PFN-0.3BDF i 0.9PFN-0.1BDF dla 10 kHz.

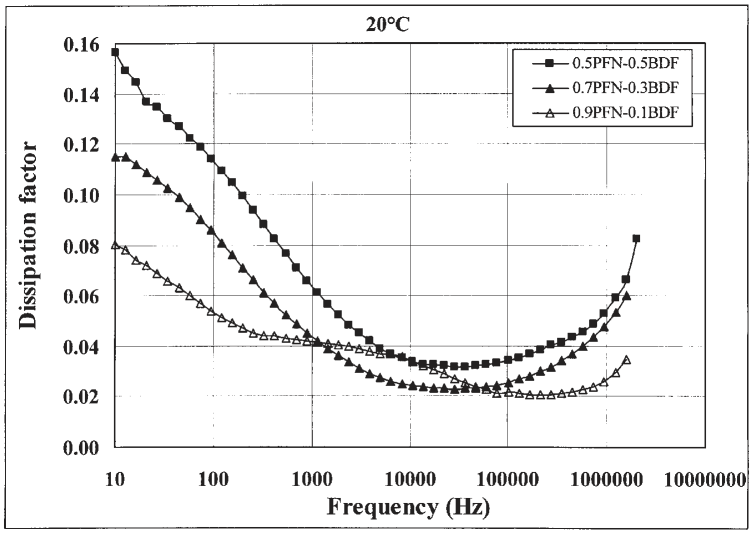

Fig. 3. Comparison of dissipation factors for 0.5PFN-0.5BDF, 0.7PFN-0.3BDF and 0.9PFN-0.1BDF thick films at 20°C.
Rys. 3. Porównanie współczynników stratności dla grubych warstw 0.5PFN-0.5BDF, 0.7PFN-0.3BDF i 0.9PFN-0.1BDF w temperaturze 20°C.

Two broad maxima in ε'= f(T) plots were observed in the examined temperature range for all compositions (Fig. 1). The first flat ε' maximum or step corresponding to the value of 1000 - 4000, which occurs at 60 – 120°C, may be ascribed to the diffuse ferroelectric transition. The second higher peak located in the temperature range 270 – 320°C is due to dielectric relaxation.

In Fig. 4a the real part of permittivity for 0.7PFN-0.3BDF thick film is depicted as a function of temperature in the range from -55 to 400°C for a few fixed frequencies. Fig. 4b presents ε' versus frequency in the temperature range from -40 to 170°C.

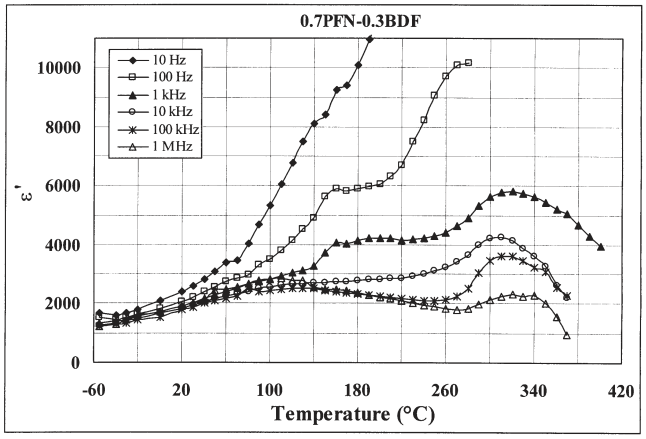

(a)

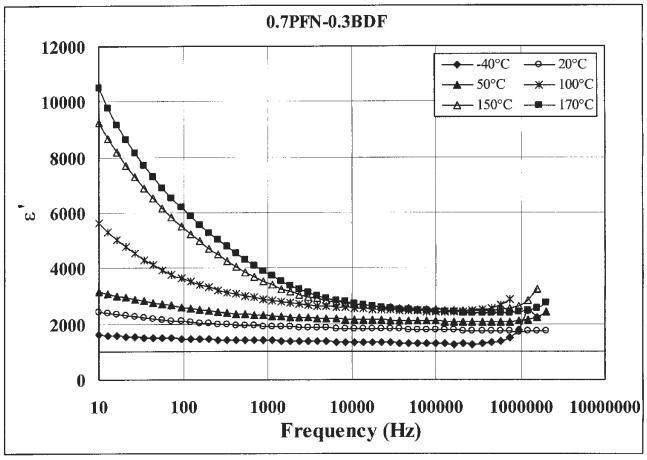

(b)

Fig. 4. Real part of permittivity for 0.7PFN-0.3BDF thick film: (a) versus temperature at frequencies 10 Hz –1 MHz in the temperature range from -40 to 400°C, (b) versus frequency in the temperature range from -40 to 170°C.

Rys. 4. Część rzeczywista przenikalności dla warstw grubych 0.7PFN-0.3BDF: (a) w funkcji temperatury w zakresie od -40 do 400°C dla częstotliwości 10 Hz –1 MHz, (b) w funkcji częstotliwości w zakresie temperatur od -40 do 170°C.

The highest dielectric permittivity values reaching 4000 in the temperature range from -55 to 150°C were attained for the 0.9PFN-0.1BDF composition, as illustrated in Fig. 5. In the range 100 Hz – 1 MHz weak frequency dependences of ε'values are observed.

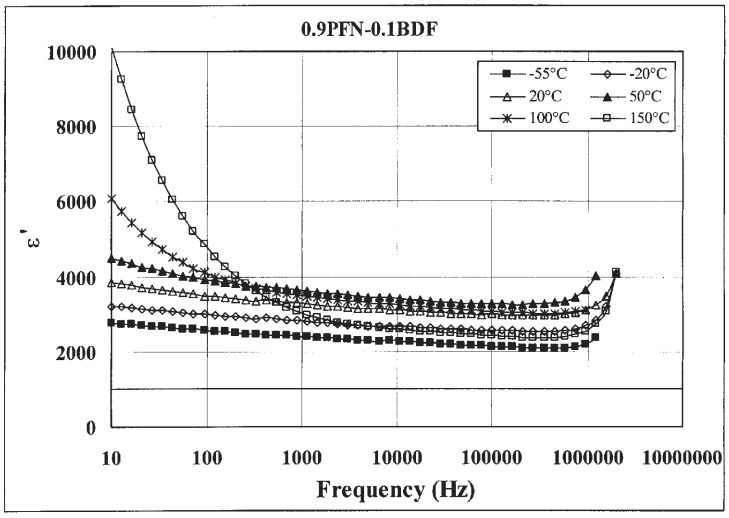

Fig. 5. Frequency dependence of the real part of permittivity for 0.9PFN-0.1BDF thick film in the temperature range from -55 to 150°C.
Rys. 5. Zależność rzeczywistej części przenikalności od częstotliwości dla warstwy warstwy 0.9PFN-0.1BDF thick film w zakresie temperatur od -55 to 150°C.

The most advantageous flat course of the ε'= *f*(T) curve over a wide temperature range was found for 0.7PFN-0.3BDF thick film (Fig. 1). This composition exhibits relatively low values of TCC, fulfilling X7U (-55÷125°C, -56%<TCC<+33%) and Z5S specifications (10-85°C, -22%<TCC<+22%) according to EIA standards. Dissipation factor at 20°C at 1 kHz is 0.04 for 0.7PFN-0.3BDF and 0.9PFN-0.1BDF and 0.06 for 0.5PFN-0.5BDF thick films, respectively (Fig. 3). Among the three studied compositions, 0.5PFN-0.5BDF thick films are characterized by the worst properties – the high temperature coefficient of capacitance, the highest dissipation factor and the lowest dielectric permittivity in the temperature range from -55 to 150°C.

In Figs. 6a – 6b frequency dependences of the real and the imaginary part of impedance are presented for 0.9PFN-0.1BDF thick film in the temperature range from -55 to 450°C. Low frequency broad plateaus in the real part Z' and maxima in the imaginary part of impedance Z" versus frequency plots are observed, shifting to higher frequencies with increasing temperature. In Fig. 7 the imaginary versus the real part of impedance for this layer is plotted in log-log coordinates for the

whole studied temperature range. The presented results indicate that in the examined frequency and temperature range one distinct dielectric response is observed, attributed to grains.

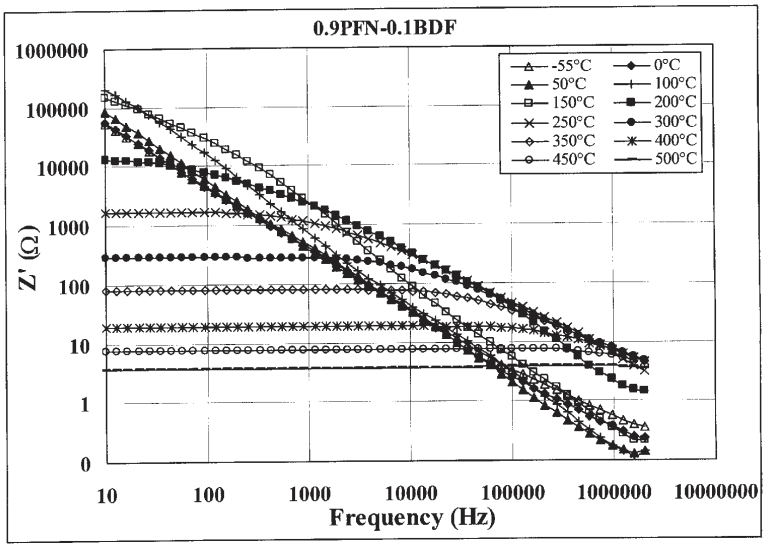

(a)

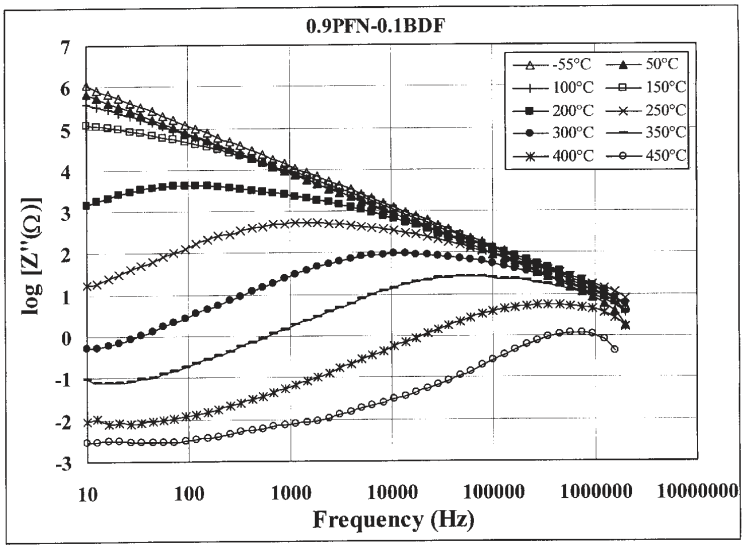

(b)

Fig. 6. Frequency dependence of the real part (a) and imaginary part (b) of impedance for 0.9PFN-0.1BDF thick film in the temperature range from -55 to 450°C.
Rys. 6. Zależność od częstotliwości rzeczywistej (a) i urojonej (b) części impedancji dla warstwy grubej 0.9PFN-0.1BDF w zakresie temperatur od -55 do 450°C.

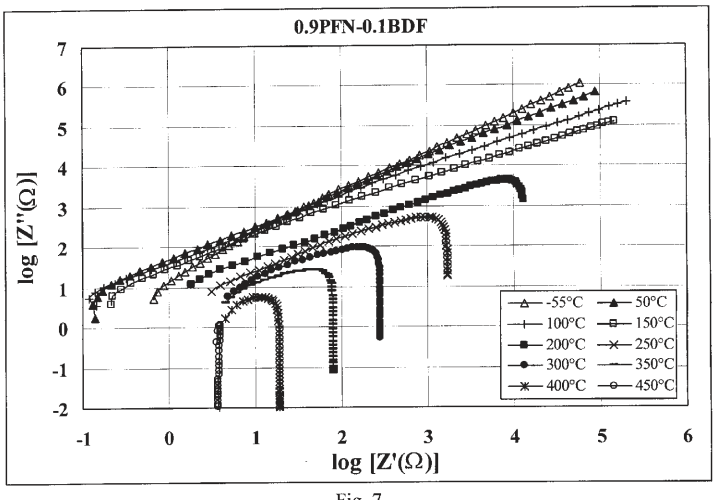

Fig. 7. Imaginary versus real part of impedance in log-log coordinates for 0.9PFN-0.1BDF thick film in the temperature range from -55 to 450°C.
Rys. 7. Zależność urojonej od rzeczywistej części impedancji w układzie współrzędnych log--log dla warstwy grubej 0.9PFN-0.1BDF w zakresie temperatur od -55 to 450°C.

As displayed in Fig. 8 for 0.7PFN-0.3BDF thick film, there occurs a single arc (or its part) at a given temperature in the complex plane impedance plots Z" = f(Z'), which may be ascribed to grains. This arc diminishes and shifts to higher frequencies with increasing temperature due to decreasing resistances of grains.

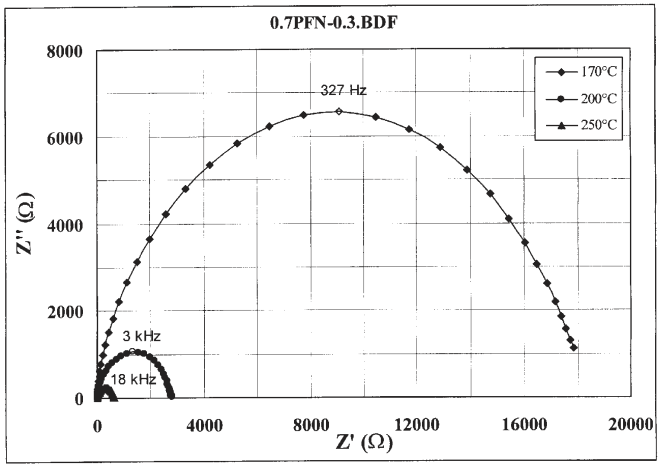

Fig. 8. Complex plane impedance plot for 0.7PFN-0.3BDF thick film at 170, 200 and 250°C.
Rys. 8. Wykres zespolonej impedancji dla warstwy grubej 0.7PFN-0.3BDF dla temperatur 170, 200 i 250°C.

Analogous complex plane impedance plots, consisting of a single arc, are obtained for 0.5PFN-0.5BDF and 0.7PFN-0.3BDF thick films. The maxima of Z" = f(Z') arcs decrease and shift to higher frequencies with increasing BDF content, as illustrated in Fig.9 at 170°C. However, these differences are significant only for 0.9PFN-0.1BDF layers, the plots being quite similar for 0.5PFN-0.5BDF and 0.7PFN-0.3BDF compositions.

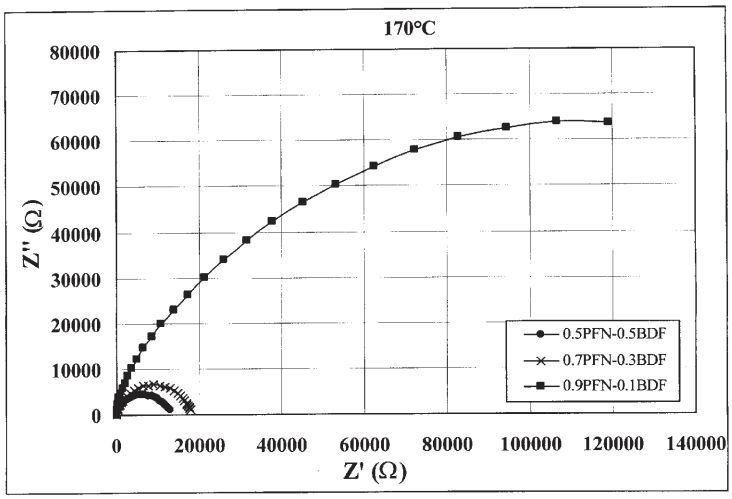

Fig. 9. Comparison of complex plane impedance plots at 170°C for 0.5PFN-0.5BDF, 0.7PFN-0.3BDF and 0.9PFN-0.1BDF thick films.
Rys. 9. Porównanie wykresów zespolonej impedancji w temperaturze 170°C dla warstw grubych 0.5PFN-0.5BDF, 0.7PFN-0.3BDF i 0.9PFN-0.1BDF.

The relevant relaxation times, estimated on the basis of frequencies corresponding to the maxima in the complex plane impedance plots ($\tau = 1/(2\pi f_{max})$), at 170°C decrease from 10^{-2} s for 0.9PFN-0.1BDF to $5x10^{-4}$ s for 0.5PFN-0.5BDF and 0.7PFN-0.3BDF thick films.

Resistivities of grains of the investigated compositions, estimated on the basis of the intercepts of the arcs with Z' axis, decrease from 10^{10} to 10^{2} Ωcm in the temperature range 20-400°C An exemplary Arrhenius plot for resistances of grains for 0.7PFN-0.3BDF layer is depicted in Fig. 10. Activation energies are 0.84, 0.87 and 0.93 eV for 0.5PFN-0.5BDF, 0.7PFN-0.3BDF and 0.9PFN-0.1BDF thick films, respectively.

As shown in Fig. 11, temperature dependence of dc conductivities of the investigated layers follows approximately the Arrhenius law. The activation energies of electrical conduction determined from the slopes of these plots are 0.66, 0.76 and 0.73 eV for 0.5PFN-0.5BDF, 0.7PFN-0.3BDF and 0.9PFN-0.1BDF thick films, re-

spectively. These values are close, although lower than the activation energies of resistances of grains, estimated on the basis of the complex plane impedance plots.

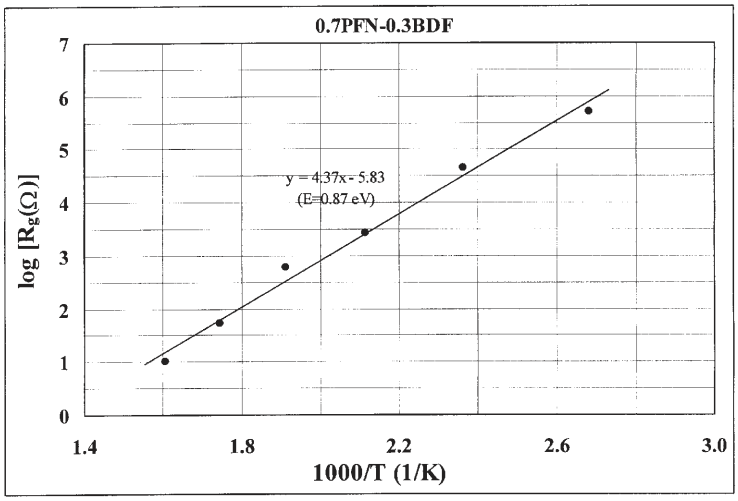

Fig. 10. Resistances of grains for 0.7PFN-0.3BDF thick film versus reciprocal temperature.
Rys. 10. Rezystancja ziaren dla warstwy grubej 0.7PFN-0.3BDF w funkcji odwrotności temperatury.

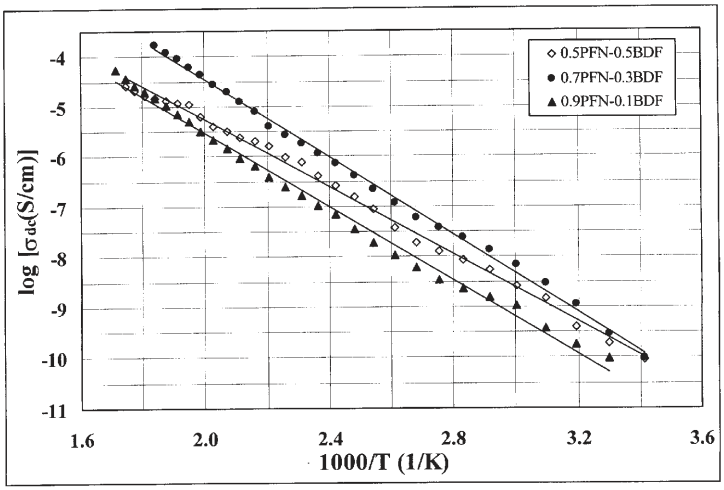

Fig. 11. Arrhenius plots of dc conductivity for 0.5PFN-0.5BDF, 0.7PFN-0.3BDF and 0.9PFN-0.1BDF thick films in the temperature range 20 - 400°C.
Rys. 11. Wykresy Arrheniusa przewodnictwa dc dla warstw grubych 0.5PFN-0.5BDF, 0.7PFN-0.3BDF i 0.9PFN-0.1BDF w zakresie temperatur 20 - 400°C.

Fig. 12 presents the fractured cross-section of a thick film capacitor based on 0.7PFN-0.3BDF composition. The dielectric layer shows relatively dense, fine-grained microstructure and its cooperation with Ag electrodes is good.

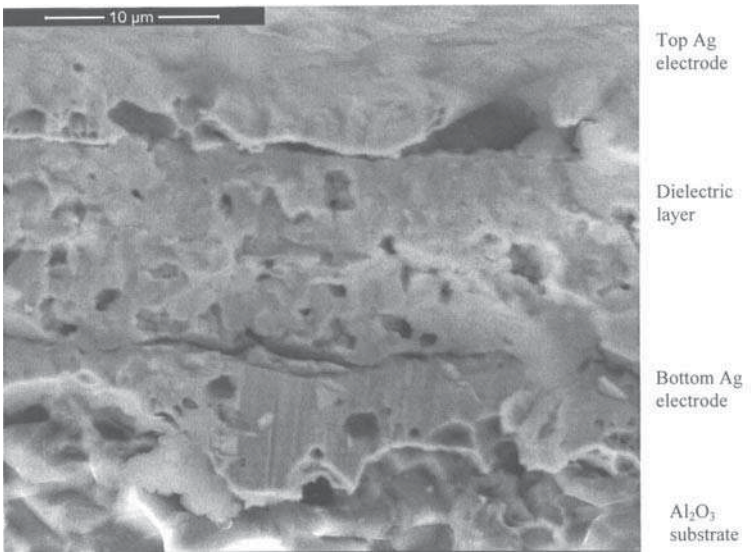

Fig. 12. SEM micrograph of the fractured cross-section of thick film capacitor with 0.7PFN-0.3BDF dielectric layer
Rys. 12. Obraz z mikroskopu skaningowego przełamu grubowarstwowego kondensatora z warstwą dielektryczną 0.7PFN-0.3BDF

Combining two single-phase multiferroic compounds $Pb(Fe_{1/2}Nb_{1/2})O_3$ and $BiFeO_3$ seems to be advantageous for thick film applications. $BiFeO_3$ addition lowers the sintering temperature, too high for pure PFT, to a level typical of conventional thick film firing procedure. Owing to the ferroelectric transition temperature for PFN (112°C) being much lower than that for $BiFeO_3$ (827°C), broad maxima in permittivity versus temperature plot for the investigated solid solutions are situated not far from the room temperature. Both doping of PFN with MnO_2 and $BiFeO_3$ with Dy_2O_3 contribute to enhancement of resistivity and suppressing of dissipation factor to an acceptable level.

4. CONCLUSION

Multiferroic perovskite solid solutions of relaxor $Pb(Fe_{1/2}Nb_{1/2})O_3$ and $Bi_{0.95}Dy_{0.05}FeO_3$ fabricated in this work and applied as dielectric layers in thick film

capacitors exhibit high dielectric permittivity reaching 2000 - 4000 in the temperature range from -55 to 150°C at 1 kHz. The most advantageous properties are shown by the 0.7PFN-0.3BDF and 0.9PFN-0.1BDF compositions, characterized by dense microstructure, high permittivity and relatively low values of temperature coefficient of capacitance and dissipation factor.

ACKNOWLEDGEMENTS

This work has been supported by Polish Ministry of Science and Higher Education under grant No. N N507 347335.

REFERENCES

[1] Gajek M., Bibes M., Fusil S., Bouzehouane K., Fontcuberta J., Barthelemy A., Fert A.: Tunnel junctions with multiferroic barriers, *Nature Materials,* 6, (2007), 296–302

[2] Scott J.F.: New developments on FRAMs: [3D] structures and all-perovskite FETs, *Materials Science and Engineering B,* 120, (2005), 6–12

[3] Qu W., Tan X., McCallum R.W., Cann D.P., Ustundag E.: Room temperature magnetoelectric multiferroism through cation ordering in complex perovskite solid solutions, *J. Phys.: Condens. Matter,* 18, (2006), 8935–8942

[4] Choudhary R.N.P., Pradhan D.K., Bonilla G.E., Katiyar R.S.: Effect of La-substitution on structural and dielectric properties of $Bi(Sc_{1/2}Fe_{1/2})O_3$ ceramics, *J. Alloys Comp.,* 437, (2007), 220-224

[5] Yuan G.L., Or S.W., Liu J.M., Liu Z.G.: Structural transformation and ferroelectromagnetic behavior in single-phase $Bi_{1-x}Nd_xFeO_3$ multiferroic ceramics, *Appl. Phys. Lett.,* 89, (2006), 052905

[6] Zhang S.T., Zhang Y., Lu M.H., Du C.L., Chen Y.F., Liu Z.G., Zhu Y.Y., Ming N.B.: Substitution – induced phase transition and enhanced multiferroic properties of $Bi_{1-x}La_xFeO_3$ ceramics, *Appl. Phys. Lett.,* 88, (2006), 162901

[7] Bhat V.V., Ramanujachary K.V., Lofland S.E., Umarji A.M.: Tuning the multiferroic properties of $Pb(Fe_{1/2}Nb_{1/2})O_3$ by cationic substitution, *J. Magnetism and Magnetic Mat.,* 280, (2004), 221-226

[8] Falqui A., Lampis N., Geddo-Lehmann A., Pinna G.G.: Low-temperature magnetic behavior of perovskite compounds $PbFe_{1/2}Ta_{1/2}O_3$ and $PbFe_{1/2}Nb_{1/2}O_3$, *J. Phys. Chem. B,* 109, (2005), 22967-22970

[9] Choudhary R.N.P., Rodriguez C., Bhattacharya P., Katiyar R.R.S., Rinaldi C.: Low frequency dielectric dispersion and magnetic properties of La, Gd modified $Pb(Fe_{1/2}Ta_{1/2})O_3$ multiferroics, *J. Magnetism and Magnetic Materials*, 313, (2007), 253-260

[10] Ivanov S.A., Nordblad P., Tellgren R., Ericsson T., Rundlof H.: Structural, magnetic and Mössbauer spectroscopic investigations of the magnetoelectric relaxor $Pb(Fe_{0.6}W_{0.2}Nb_{0.2})O_3$, *Sol. Stat. Sci*., 9, (2007), 440-450

[11] Stoch A., Kulawik J., Stoch P., Maurin J., Zachariasz P., Structural, electrical and Mössbauer effect studies of and $0.5Bi_{0.95}Dy_{0.05}FeO_3$-$0.5Pb(Fe_{0.5}Nb_{0.5})O_3$ multiferroics, OSSM2008 Conf., Koninki, 8–11.06.2008, *Acta Physica Polonica* A, in press

WŁAŚCIWOŚCI DIELEKTRYCZNE PEROWSKITOWYCH MULTIFERROICZNYCH GRUBYCH WARSTW $Pb(Fe_{0.5}Nb_{0.5})O_3$-$Bi_{0.95}Dy_{0.05}FeO_3$

W artykule opisano przygotowanie i nanoszenie dielektrycznych grubych warstw wykazujących multiferroiczne właściwości. Opracowane warstwy oparte są na dwóch multiferroicznych związkach o strukturze perowskitu – relaksorze $Pb(Fe_{0.5}Nb_{0.5})O_3$ i $Bi_{0.95}Dy_{0.05}FeO_3$. Badano zespoloną impedancję i przenikalność elektryczną grubych warstw w funkcji temperatury (od -55 do 450°C) i częstotliwości (10 Hz – 2 MHz). Mierzono przewodnictwo dc w zakresie temperatur 20 - 400°C. Badano mikrostrukturę próbek przy użyciu mikroskopu skaningowego. Na wykresach zespolonej impedancji w danej temperaturze istnieje pojedynczy łuk, związany z ziarnami, który zmniejsza się i przesuwa w stronę wyższych częstotliwości ze wzrostem temperatury. Maksymalne wartości przenikalności elektrycznej badanych warstw wynoszą 2000 – 4000 w zakresie temperatur od -55 do 150°C dla 1 kHz. W zakresie temperatur od -55 do 450°C występują dwa szerokie maksima ε' przypisywane przemianie ferroelektrycznej i relaksacji dielektrycznej. Korzystnymi cechami opracowanych kompozycji są: niska temperatura spiekania odpowiednia dla konwencjonalnej procedury grubowarstwowej, zwarta mikrostruktura i wysoka przenikalność elektryczna słabo zmieniająca się w szerokim zakresie częstotliwości i temperatur.